

# Kidney360

## The Role of High-Frequency Wall Vibrations in Adverse Vascular Remodeling of Arteriovenous Fistula for Hemodialysis --Manuscript Draft--

<b>Manuscript Number:</b>	K360-2025-001100R1
<b>Full Title:</b>	The Role of High-Frequency Wall Vibrations in Adverse Vascular Remodeling of Arteriovenous Fistula for Hemodialysis
<b>Short Title:</b>	High-Frequency Vibrations and Vascular Remodeling in AVFs
<b>Article Type:</b>	Original Research
<b>Section/Category:</b>	Dialysis
<b>Corresponding Author:</b>	Michela Bozzetto Istituto di Ricerche Farmacologiche Mario Negri Bergamo, Bergamo ITALY
<b>Corresponding Author E-Mail:</b>	michela.bozzetto@marionegri.it
<b>Other Authors:</b>	Luca Soliveri, PhD Sofia Poloni, MS Paolo Brambilla, MD Simona Zerbi, MD Giulia Cabrini, MS Anna Caroli, PhD Andrea Remuzzi, EngD Kristian Valen-Sendstad, PhD
<b>Order of Authors (with Contributor Roles):</b>	Luca Soliveri, PhD (Investigation; Methodology; Software; Writing – original draft; Writing – review & editing) Sofia Poloni, MS (Methodology; Software; Writing – review & editing) Paolo Brambilla, MD (Data curation; Investigation; Writing – review & editing) Simona Zerbi, MD (Data curation; Investigation; Writing – review & editing) Giulia Cabrini, MS (Investigation; Software; Writing – review & editing) Anna Caroli, PhD (Supervision; Writing – review & editing) Andrea Remuzzi, EngD (Conceptualization; Investigation; Methodology; Supervision; Writing – review & editing) Kristian Valen-Sendstad, PhD (Conceptualization; Methodology; Software; Supervision; Writing – original draft) Michela Bozzetto, PhD (Conceptualization; Data curation; Investigation; Methodology; Supervision; Writing – original draft)
<b>Manuscript Classifications:</b>	3: Access Blood Flow; 31: Arteriovenous Fistula; 43: Cardiovascular Disease; 72: Chronic Kidney Disease; 121: Dialysis Access; 196: Hemodialysis Access; 424: Vascular Access; 470: Biomarkers; 478: Imaging
<b>Abstract:</b>	Background. Despite progress in research, the mechanobiological mechanisms behind adverse vascular remodeling and failure in arteriovenous fistulae (AVF) for hemodialysis remain unclear. The aim of this investigation is to assess the association between flow-induced vascular wall vibrations and adverse vascular remodeling in AVFs. Methods. Six end-stage kidney disease patients with native distal radio-cephalic AVF were monitored for 1 year with magnetic resonance imaging and Doppler ultrasound examinations. Patients were divided based on AVF outcomes: two maintained proper

	<p>AVF patency and four developed complications (two venous stenoses and two excessive dilations). Patient-specific fluid-structure interaction simulations were performed at different time points.</p> <p>Results. Before vascular remodeling, stenotic AVFs exhibited two dominant frequency bands, between 45 and 100 Hz, while excessively dilated AVFs exhibited a single band at 50 Hz. Before the onset of remodeling, patients with complications exhibited significantly higher vibration amplitude (<math>22.5 \pm 5.8 \mu\text{m}</math> vs. <math>6.6 \pm 2.0 \mu\text{m}</math>, <math>p &lt; 0.01</math>) and high-pass strain (<math>(1.30 \pm 0.35) \cdot 10^{-3}</math> vs. <math>(0.30 \pm 0.10) \cdot 10^{-3}</math>, <math>p &lt; 0.01</math>) than those with proper patency. Significant differences in vibration amplitude and high-pass strain were observed between patients with proper patency and those with stenosis (<math>p &lt; 0.001</math> and <math>p &lt; 0.01</math>, respectively), and in high-pass strain between patients with preserved patency and those with excessive dilatation (<math>p &lt; 0.01</math>).</p> <p>Conclusions. Specific vibration frequencies and amplitude levels appear to be associated with distinct types of vascular remodeling, indicating they could potentially be biomarkers for AVF surveillance.</p>
<b>Funding Information:</b>	
<b>Additional Information:</b>	
<b>Question</b>	<b>Response</b>
Is this a Basic Science or Clinical Science topic?	Clinical Research
Clinical Trial Registration  My study was a clinical trial and is registered in one of the registries recommended by the <a href="#">International Committee of Medical Journal Editors (ICMJE)</a> .	N/A because this is not a clinical trial
Institutional Review Board or Ethics Committee Oversight  For all clinical experimentation described in this manuscript, I received approval by an Institutional Review Board or equivalent Ethics Committee and responded regarding patient consent, or I provided the reason for the exemption.	Yes
Please select a response: as follow-up to "Institutional Review Board or Ethics Committee Oversight  For all clinical experimentation described in this manuscript, I received approval by an Institutional Review Board or equivalent Ethics Committee and responded regarding patient consent, or I provided the reason for the exemption."	This study is exempt from the Institutional Review Board or Ethics Committee approval, and I have provided the reason for exemption.
Please provide the reason for exemption: as follow-up to "Please select a response:"	The 6 patients were followed in routine clinical practice at ASST Papa Giovanni XXIII. All clinical data were fully anonymized and analyzed retrospectively; therefore, no patient consent was required.
Declaration of Helsinki	N/A

<p>For all clinical experimentation described in the manuscript, I adhered to the Declaration of Helsinki and indicated my response below accordingly.</p>	
<p>Declaration of Istanbul</p> <p>My study is related to clinical organ transplantation, and the clinical and research activities being reported are consistent with the Principles of the Declaration of Istanbul as outlined in the Declaration of Istanbul on Organ Trafficking and Transplant Tourism.</p>	<p>N/A</p>
<p>Animal Experimentation</p> <p>Animal experimentation is discussed in this manuscript, and I have adhered to the NIH Guide for the Care and Use of Laboratory Animals or the equivalent.</p>	<p>N/A</p>
<p>Preprint Server</p> <p>Posting of unrefereed manuscripts to a community preprint server by the author will not be considered prior publication provided that the conditions included within the <a href="#">Instructions for Authors</a> are met. Has this paper already been posted on a preprint server such as arXiv or bioRxiv?</p>	<p>This research was not posted on a preprint server.</p>
<p>Key Points: Please state the 2-3 key points of the article. The responses included here will be included with your final published paper. The key points should be complete statements and not duplications of your keywords or index terms. At least two key points are required.</p>	<p>Key Point 1; Key Point 2; Key Point 3</p>
<p>Key point #1: as follow-up to "Key Points: Please state the 2-3 key points of the article. The responses included here will be included with your final published paper. The key points should be complete statements and not duplications of your keywords or index terms. At least two key points are required."</p>	<p>Flow-induced high-frequency vascular vibrations, computed through fluid-structure interaction simulations, are associated with fistula complications.</p>
<p>Key point #2: as follow-up to "Key Points: Please</p>	<p>The association between vibrations and arteriovenous fistula complications suggests a potential new mechanism responsible for vascular remodeling.</p>

<p>state the 2-3 key points of the article. The responses included here will be included with your final published paper. The key points should be complete statements and not duplications of your keywords or index terms. At least two key points are required."</p>	
<p>Key point #3: as follow-up to "Key Points: Please state the 2-3 key points of the article. The responses included here will be included with your final published paper. The key points should be complete statements and not duplications of your keywords or index terms. At least two key points are required."</p>	<p>The frequency and amplitude of vibrations are potential biomarkers for arteriovenous fistula surveillance.</p>
<p>Study Group:</p> <p>Does your paper include study group(s)? If yes, please provide a list of study group(s) and members that have contributed to or participated in the submitted work in some way. This list may contain either a collaboration of individuals (e.g., investigators) and/or the name of an organization (e.g., a laboratory, educational institution, corporation, or department) and its members</p>	<p>No</p>
<p>Scale of Data Generated (<i>select all that apply</i>)</p>	<p>Low-throughput experimental data (e.g., small-scale animal or cell culture studies, biochemical assays, microscopy analyses, case reports, and case series)</p>
<p>Data Availability (<i>select all that apply</i>)*<b>Additional information:</b> Original data generated for the study will be made available upon reasonable request to the corresponding author: This is not recommended for large datasets but is acceptable for low-throughput experimental data. If data are not deposited in a public access repository, or access will otherwise be subject to partial restriction, provide details in the textbox.- Data belong to a third party, and authors are not authorized to share the data: If data cannot be shared because they belong to a third party, specify the identity of the third party and reason for the</p>	<p>Original data generated for the study will be made available upon reasonable request to the corresponding author.*</p>

<p>restriction (e.g., proprietary data, administrative data governed by regulatory or legal frameworks).- Original data cannot be shared: This choice is allowable in select instances only, such as for research that applies to the <a href="#">CARE Principles — Global Indigenous Data Alliance</a>, and requires editor approval.</p>	
<p>Data Type:  as follow-up to "Data Availability (<i>select all that apply</i>)*<b>Additional information:</b>  Original data generated for the study will be made available upon reasonable request to the corresponding author: This is not recommended for large datasets but is acceptable for low-throughput experimental data. If data are not deposited in a public access repository, or access will otherwise be subject to partial restriction, provide details in the textbox.- Data belong to a third party, and authors are not authorized to share the data: If data cannot be shared because they belong to a third party, specify the identity of the third party and reason for the restriction (e.g., proprietary data, administrative data governed by regulatory or legal frameworks).- Original data cannot be shared: This choice is allowable in select instances only, such as for research that applies to the <a href="#">CARE Principles — Global Indigenous Data Alliance</a>, and requires editor approval."</p>	<p>Health Care Data; Image Data; Raw Data/Source Data; Software Executable Code</p>
<p>Reason for Restricted Access:  as follow-up to "Data Availability (<i>select all that apply</i>)*<b>Additional information:</b>  Original data generated for the study will be made available upon reasonable request to the corresponding author: This is not recommended for large datasets but is acceptable for low-throughput experimental data. If data are not deposited in a public access repository, or access will otherwise be subject to partial restriction, provide details in the textbox.- Data belong to a third party, and authors are not authorized to share the data: If data cannot be shared because they belong to a third party, specify the identity of the third party and reason for the restriction (e.g., proprietary data,</p>	<p>The data of magnetic resonance images, Doppler ultrasound examinations, and post-processing results supporting the findings of this work are fully anonymized and openly available in the Zenodo repository at 10.5281/zenodo.14754994, following a specific request to the authors.  The code used for fluid-structure interaction simulations is available in VaSP github repository at <a href="https://github.com/KVSlab/VaSP">https://github.com/KVSlab/VaSP</a>.</p>

administrative data governed by regulatory or legal frameworks).- Original data cannot be shared: This choice is allowable in select instances only, such as for research that applies to the [CARE Principles — Global Indigenous Data Alliance](#), and requires editor approval."

ACCEPTED

**OPEN**

**Kidney360 Publish Ahead of Print**

**DOI: 10.34067/KID.0000001112**

## **The Role of High-Frequency Wall Vibrations in Adverse Vascular Remodeling of Arteriovenous Fistula for Hemodialysis**

Luca Soliveri<sup>1</sup>, Sofia Poloni<sup>2</sup>, Paolo Brambilla<sup>3,4</sup>, Simona Zerbi<sup>5</sup>, Giulia Cabrini<sup>6</sup>, Anna Caroli<sup>1</sup>, Andrea Remuzzi<sup>6</sup>, Kristian Valen-Sendstad<sup>7\*</sup>, Michela Bozzetto<sup>1\*</sup>

\*Shared last coauthorship

<sup>1</sup> *Department of Bioengineering, Istituto di Ricerche Farmacologiche Mario Negri IRCCS, Bergamo, Italy*

<sup>2</sup> *Department of Engineering and Applied Sciences, University of Bergamo, Bergamo, Italy*

<sup>3</sup> *Diagnostic Radiology, ASST Papa Giovanni XXIII Hospital, Bergamo, Italy*

<sup>4</sup> *School of Medicine, University of Milano-Bicocca, Milan, Italy*

<sup>5</sup> *Nephrology and Dialysis Unit, ASST Papa Giovanni XXIII Hospital, Bergamo, Italy*

<sup>6</sup> *Department of Management, Information and Production Engineering, University of Bergamo, Bergamo, Italy*

<sup>7</sup> *Department of Computational Physiology, Simula Research Laboratory, Oslo, Norway*

**Corresponding Author:** Dr. Michela Bozzetto, Email address:

[michela.bozzetto@marionegri.it](mailto:michela.bozzetto@marionegri.it)

This is an open access article distributed under the Creative Commons Attribution License 4.0 (CC-BY), which permits unrestricted use, distribution, and reproduction in any medium, provided the original work is properly cited.

## Abstract

**Background.** Despite progress in research, the mechanobiological mechanisms behind adverse vascular remodeling and failure in arteriovenous fistulae (AVF) for hemodialysis remain unclear. The aim of this investigation is to assess the association between flow-induced vascular wall vibrations and adverse vascular remodeling in AVFs.

**Methods.** Six end-stage kidney disease patients with native distal radio-cephalic AVF were monitored for 1 year with magnetic resonance imaging and Doppler ultrasound examinations. Patients were divided based on AVF outcomes: two maintained proper AVF patency and four developed complications (two venous stenoses and two excessive dilatations). Patient-specific fluid-structure interaction simulations were performed at different time points.

**Results.** Before vascular remodeling, stenotic AVFs exhibited two dominant frequency bands, between 45 and 100 Hz, while excessively dilated AVFs exhibited a single band at 50 Hz. Before the onset of remodeling, patients with complications exhibited significantly higher vibration amplitude ( $22.5 \pm 5.8 \mu\text{m}$  vs.  $6.6 \pm 2.0 \mu\text{m}$ ,  $p < 0.01$ ) and high-pass strain ( $(1.30 \pm 0.35) \cdot 10^{-3}$  vs.  $(0.30 \pm 0.10) \cdot 10^{-3}$ ,  $p < 0.01$ ) than those with proper patency. Significant differences in vibration amplitude and high-pass strain were observed between patients with proper patency and those with stenosis ( $p < 0.001$  and  $p < 0.01$ , respectively), and in high-pass strain between patients with preserved patency and those with excessive dilatation ( $p < 0.01$ ).

**Conclusions.** Specific vibration frequencies and amplitude levels appear to be associated with distinct types of vascular remodeling, indicating they could potentially be biomarkers for AVF surveillance.

Supplemental Digital Content: <http://links.lww.com/KN9/B492>

## Introduction

Native arteriovenous fistula (AVF) is the preferred vascular access for hemodialysis<sup>1,2</sup>, though it has a failure rate of 40% within the first year after surgery<sup>3-5</sup>. The primary cause of failure is inward vascular remodeling due to intimal hyperplasia, a proinflammatory response promoting smooth muscle cell activation, proliferation, and migration in the intimal layer<sup>6-12</sup>. Moreover, excessive outward remodeling may also be associated with complications, potentially causing high flow leading to cardiac overload<sup>2,13</sup>.

In the last decades, medical image-based computational fluid dynamics<sup>14-19</sup> and fluid-structure interaction (FSI)<sup>20-24</sup> simulations have been used to investigate the abnormal blood flow conditions that arise after the creation of an arteriovenous shunt. Specifically, most research has focused on abnormal wall shear stress (WSS) on the endothelium and its role in adverse vascular remodeling. As a result, various WSS-based indices have been proposed to correlate with AVF failure. In this context, the most recent work from the Hemodialysis Fistula Maturation Consortium demonstrated that higher WSS was positively associated with subsequent lumen expansion and unassisted clinical maturation<sup>25</sup>. However, despite the increased understanding gained from these studies on the hemodynamic characterization of AVFs, a clear correlation between these indices and pathological vascular remodeling has not yet been established<sup>26</sup>, limiting the effectiveness of using WSS as a biomarker or predictor of disease progression in clinical contexts.

Interestingly, recent FSI studies on patient-specific AVF models from our group revealed the occurrence of flow-induced vascular wall vibrations in the AVF vein<sup>27,28</sup>, suggesting that these vibrations may play a role in adverse vascular remodeling<sup>29</sup>. Additionally, we showed that AVFs characterized by significant adverse vascular remodeling exhibited high-frequency components in AVF sounds recorded with a stethoscope<sup>30,31</sup>. We have also recently reviewed

the existing literature on the biological effects of wall vibrations and shown that high-frequency mechanical stimuli may influence vascular cells' mechanobiology, leading to both morphological and functional changes<sup>32</sup>.

Therefore, the current work aimed to investigate the effects of flow-induced vascular wall vibrations on vascular remodeling in six patients with native distal radio-cephalic AVFs over a 1-year follow-up period after surgical creation.

## Methods

This report describes six patients with end-stage kidney disease (five males and one female;  $54 \pm 20$  years) who underwent native radio-cephalic AVF creation in the forearm and were followed in routine clinical practice at the Nephrology and Dialysis Unit of ASST Papa Giovanni XXIII. Patients with a previously failed native AVF or graft in the same arm were not included. All collected clinical data were fully anonymized and analyzed retrospectively. Clinical characteristics of the patients are summarized in **Table 1**.

Magnetic resonance imaging (MRI), Doppler ultrasound (DUS), and FSI simulations were performed at three time points: within 3 days of AVF creation, at AVF maturation (around 6 weeks post-surgery), and 1 year post-surgery. For two patients, additional MRI and DUS data were collected at 6 months post-surgery (**Figure 1a**).

For the analysis of the FSI results, patients were retrospectively divided into three groups based on AVF outcome, assessed by clinical evaluation, which included DUS assessments and any reported AVF complications. Specifically, the AVF outcomes considered were: proper patency (P) maintained over time, stenosis (S) formation, and excessive dilatation (D), defined as a cephalic vein diameter exceeding twice the recommended<sup>2</sup> diameter of 6 mm.

Computed hemodynamic patterns and vascular wall vibrations were analyzed in relation to vascular wall remodeling and AVF outcomes over time.

### ***Medical imaging acquisition***

The complete FSI pipeline is illustrated in **Figure 1b**. Non-contrast-enhanced MRI were acquired using a 1.5T scanner, covering an arm region extending approximately 5 cm above and 3 cm below the anastomosis. A detailed description of the MRI protocol can be found in our previous publications<sup>33–35</sup>. Prior to each MRI scan, a DUS examination of the AVF was performed to measure vessel diameters and blood flow velocities in the brachial and radial arteries.

### ***FSI simulations***

MRI-based 3D AVF surfaces were used to generate meshes consisting of approximately 200,000 tetrahedral elements, building upon a previous mesh refinement study<sup>28</sup>. FSI simulations of the blood flow were performed using turtleFSI solver<sup>36</sup>, including compliant vascular wall and perivascular tissue modeling. A simulation timestep of 0.1 ms was selected to accurately capture high-frequency fluctuations in velocity and pressure<sup>37</sup>. Patient-specific flow waveforms obtained from DUS measurements were imposed at the inlet of the proximal and distal radial artery. The simulations accounted for the distinct mechanical properties of the vein and artery, as well as the stiffening and thickening of the cephalic vein during maturation<sup>38</sup>. The viscoelastic effect of perivascular tissue was modeled with Robin boundary conditions<sup>39</sup>. For further details on the FSI pipeline, please refer to **Supplemental Material** and our recent publication<sup>28</sup>.

### ***Post-processing of the results***

The Q-Criterion was employed to highlight vortices and flow instabilities<sup>28</sup>. Fluid velocity and wall displacement spectrograms were generated to illustrate the evolution of high-frequency content over the cardiac cycle<sup>40,41</sup>. Vibration and high-pass displacement amplitudes were calculated by high-pass filtering the vascular wall deformations over 25 Hz<sup>28</sup>. The pointwise 99<sup>th</sup> spatial percentile<sup>41</sup> of vibration was used to represent the vibration amplitude progression over time.

Cross-sectional slices of time-averaged vibration amplitude and high-pass strain surface maps were extracted at the time point preceding the main vascular remodeling event ( $t-1$ ) (e.g., stenosis formation or excessive dilatation) to investigate how these metrics influenced subsequent vascular remodeling at the following timestep. Slices were taken perpendicular to the model's centerlines within the first 2.5 cm of the juxta-anastomotic vein (JAV), with a spacing of 0.1 mm. The average value of each metric was obtained for each slice and considered for statistical analysis, resulting in 25 values per patient.

The average values of common WSS indices in the JAV—time-averaged WSS (TAWSS), oscillatory shear index (OSI), and spectral power index (SPI), a proposed metric of cycle-invariant turbulent-like flow<sup>42</sup>—were computed from FSI simulations to explore their relationship with wall vibrations.

### ***Statistical analysis***

Statistical analysis was conducted using R software (version 4.1.0). Values of vibration amplitude and high-pass strain at time  $t-1$  were considered for the analysis to assess their impact on subsequent vascular remodeling. Boxplots were generated to compare the distribution of vibration amplitude and high-pass strain in patients with proper patency and in those experiencing complications. A linear mixed-effects model was fitted using the *lmer*

function from the *lme4* package, with ‘Vibration amplitude’ and ‘High-pass strain’ as response variables, group (‘Patency’, ‘Stenosis’, and ‘Dilatation’) as fixed effect, and ‘Patient’ as random effect to account for repeated measures within subjects. A Shapiro-Wilk test was performed to assess the normality of the residuals. Where there was a violation of the normality assumptions, a generalized linear mixed model was subsequently fitted using the *glmmTMB* package, with a Gamma distribution and a log link function. The significance level was set at 0.05 when examining differences between patients with proper patency and those with complications (‘Patency’ vs. ‘Adverse Remodeling’), while for comparisons among the three groups (‘Patency’, ‘Stenosis’, and ‘Dilatation’), the Bonferroni correction was applied, adjusting the significance level to  $\alpha = \frac{0.05}{3} = 0.0167$  to account for multiple testing.

Finally, we explore the correlation between WSS indices (TAWSS, OSI, SPI) and wall vibrations and high-pass strain using linear mixed-effects models. Patient identity was included as a random effect to account for repeated measures within subject. The relationships were also evaluated after log<sub>10</sub>-transformation of vibration metrics to account for potential nonlinear scaling. The conditional correlation coefficient (R) and significance levels were calculated, and results were visualized using scatter plots with the model regression line.

## Results

### *Evolution in AVF morphology and blood flow vs AVF outcome*

The six AVFs followed in this investigation had different clinical evolutions and underwent diverse types of remodeling (see **Figure 2**). The pre-operative diameters of all of the radial arteries and cephalic veins were greater than 2 mm, which is the suggested threshold for creating a proper vascular access <sup>2</sup>. In all patients, the creation of the arteriovenous shunt

resulted in a sudden increase in blood flow rates and vessel diameter, particularly of the cephalic vein, already 3 days after surgery, compared to pre-operative measurements. All AVFs then experienced proper maturation, achieving a cephalic vein diameter of at least 6 mm, sufficient for successful cannulation <sup>2</sup>, and a blood flow rate adequate for initiating hemodialysis (see **Figure 3**).

Patients P1 and P2 maintained AVF patency at the 1-year follow-up, with cephalic vein diameters remaining almost unchanged (7.2 mm and 8.4 mm at 1 year, respectively) and stable blood flow in the brachial artery over time (cycle-averaged blood flow volumes of 527 mL/min for P1 and 840 mL/min for P2 at 1 year), enabling them to continue hemodialysis. In contrast, patients S1 and S2 developed stenosis in the JAV, leading to significant narrowing of the cephalic vein, with diameters returning approximately to pre-operative values (minimum diameters of 2.0 mm and 3.5 mm, respectively, at 1 year) and a decrease in brachial blood flow rate (from 992 to 860 mL/min in S1 and from 1101 to 777 mL/min in S2). Both patients experienced later AVF failure after the last follow-up of the current work. On the contrary, patients D1 and D2 experienced excessive vein dilatation, with diameters increasing to more than twice the recommended clinical guideline size of 6 mm. D1 exhibited uniform vein dilatation (up to 14.8 mm in diameter) starting at anastomosis, whereas for D2 the diameter of the juxta-anastomotic segment remained unchanged but the patient developed significant dilatation at the vein curvature (up to 13.1 mm in diameter). The increase in vessel diameter was accompanied by an increase in brachial blood flow volume in both patients (from 577 mL/min to 1545 mL/min in D1, and from 403 mL/min to 801 mL/min in D2). Patient D1 continued on hemodialysis and later underwent a kidney transplantation. Patient D2 experienced AVF closure due to a thrombus caused by hypotension a few weeks after the last follow-up and AVF patency was restored using a Fogarty procedure. After the transplant, this

AVF experienced further dilatation and an increase in blood flow and was closed due to a high risk of cardiac overload.

### ***High-frequency wall vibrations and AVF outcome***

Patients P1 and P2, who experienced good patency over time, exhibited minor flow instabilities at the anastomosis and within the JAV. As a result, the fluid velocity and wall displacement spectrograms (see **Figure 4**) show negligible vibrations, with frequencies and amplitudes progressively decreasing over time. Consistently, the pointwise vibration amplitudes shown in **Figure 5** remained low and gradually decreased over time as well.

In contrast, patients who developed complications exhibited higher vibration frequencies and amplitudes. Stenotic patients S1 and S2 exhibited elevated Q-Criterion levels in the JAV segment, indicating a strong deviation from laminar to transitional flow. This altered flow pattern resulted in high-frequency fluctuations in blood flow velocity and vein wall displacement, as illustrated in the spectrograms (see **Figure 4**). Patient S1 demonstrated the highest frequency fluctuations after AVF maturation, which persisted up to the 1-year follow-up. These fluctuations reached up to 800 Hz, with amplitudes ranging from -8 to -6 dB at the systolic peak for fluid velocity, and up to 700 Hz with amplitudes between -28 and -22 dB for wall displacement. Similarly, Patient S2 exhibited velocity fluctuations up to 500 Hz and wall displacement fluctuations up to 350 Hz at 6 months, which decreased following the development of stenosis at 1 year. Notably, both patients exhibited two distinct high-frequency bands in the displacement spectrogram prior to the onset of stenosis, with the lower-frequency band showing the highest vibration amplitude: 55-65 Hz and around 100 Hz for S1, and 45-50 Hz and 70-75 Hz for S2. After stenosis developed, these bands persisted but shifted to slightly higher frequencies and lower amplitudes. This pattern is further confirmed by the pointwise vibration data (see **Figure 5**), which shows the highest

amplitudes before stenosis onset (S1: peak = 100  $\mu\text{m}$ , cycle-average = 64  $\mu\text{m}$ ; S2: peak = 65  $\mu\text{m}$ , cycle-average = 36  $\mu\text{m}$ ), followed by a decrease after stenosis development (S1: peak = 52  $\mu\text{m}$ , cycle-average = 25  $\mu\text{m}$ ; S2: peak = 24  $\mu\text{m}$ , cycle-average = 12  $\mu\text{m}$ ), though the values remained relatively elevated.

As regards patients who experienced excessive venous dilatation, high-flow instabilities were already observed near the anastomosis in patient D1 after AVF creation. As a result, velocity fluctuations up to 450 Hz were detected immediately after AVF surgery, persisting throughout the maturation period (see **Figure 4**). Low-amplitude wall vibrations (around -28 dB) were observed up to 600 Hz, with a prominent frequency band (exceeding -22 dB) consistently detected at around 50 Hz during the maturation phase. Notably, this high-frequency content was suppressed following significant dilatation of the JAV at 1 year. Consistently, the highest pointwise vibration amplitudes were observed at the time of maturation (peak = 84  $\mu\text{m}$ , cycle-average = 46  $\mu\text{m}$ ), and became almost negligible after remodeling (see **Figure 5**). In contrast, Patient D2 exhibited a different progression. Initially, negligible flow instabilities and no vibrations were observed immediately after surgery. However, after AVF maturation, flow instabilities arose at the JAV curvature, leading to a gradual increase in both velocity and displacement frequencies, reaching up to 300 Hz at 1 year. As in the previous case, the most prominent vibration mode detected was at around 50 Hz. This trend, with increasing vibrations from post-surgery through maturation to the 1-year follow-up, was also reflected in the vibration amplitudes, with the highest values recorded at 1 year (peak = 77  $\mu\text{m}$ , cycle-average = 37  $\mu\text{m}$ ).

The statistical analysis of the cross-sectional slices extracted at time point t-1, as shown in **Figure 6**, revealed that patients in the 'Patency' group exhibited significantly lower variability in vibration amplitude and high-pass strain compared to the 'Stenosis' and 'Dilatation' groups, and markedly lower values that were more closely clustered around the

median. The generalized linear mixed model on the cross-sectional slices revealed significant differences in time-averaged vibration amplitudes ( $6.6 \pm 2.0 \mu\text{m}$  vs.  $22.5 \pm 5.8 \mu\text{m}$ ,  $p < 0.01$ ) and high-pass strain ( $(0.30 \pm 0.10) \cdot 10^{-3}$  vs.  $(1.30 \pm 0.35) \cdot 10^{-3}$ ,  $p < 0.01$ ) between patients with proper patency and those with complications ('Adverse Remodeling'). Moreover, further distinguishing between 'Stenosis' and extreme 'Dilatation', a significant difference in vibration amplitude was confirmed between the 'Patency' and 'Stenosis' groups ( $6.6 \pm 2.0 \mu\text{m}$  vs.  $31.7 \pm 9.7 \mu\text{m}$ ,  $p < 0.001$ ), while the difference between 'Patency' and 'Dilatation' was not significant after Bonferroni correction ( $6.6 \pm 2.0 \mu\text{m}$  vs.  $15.9 \pm 4.8 \mu\text{m}$ ,  $p > 0.0167$ ). Regarding high-pass strain, a significant difference was confirmed between the 'Patency' and 'Stenosis' groups ( $(0.30 \pm 0.10) \cdot 10^{-3}$  vs.  $(1.68 \pm 0.58) \cdot 10^{-3}$ ,  $p < 0.01$ ) as well as between the 'Patency' and 'Dilatation' groups ( $(0.30 \pm 0.10) \cdot 10^{-3}$  vs.  $(1.00 \pm 0.35) \cdot 10^{-3}$ ,  $p < 0.0167$ ).

#### ***Relation between conventional hemodynamics and vibrations***

The correlation analysis between hemodynamics and vibrations is reported in **Figure 7**. For vibration amplitude, only SPI exhibited a strong and highly significant correlation ( $R = 0.75$ ,  $p < 0.001$ ), whereas TAWSS and OSI showed low-to-moderate correlations ( $R = 0.53$ ,  $p < 0.05$ ;  $R = 0.49$ ,  $p < 0.05$ , respectively). For high-pass strain, TAWSS exhibited a low-to-moderate significant correlation ( $R = 0.46$ ,  $p < 0.05$ ), OSI was not significantly associated ( $R = 0.35$ ,  $p > 0.05$ ), and SPI again showed a strong and highly significant correlation ( $R = 0.66$ ,  $p < 0.001$ ). When applying a logarithmic transformation to vibration metrics, the correlations with SPI slightly improved ( $R = 0.80$  and  $R = 0.70$ ;  $p < 0.001$ ). Correlations with TAWSS and OSI remained unchanged. For clarity, only the SPI-related plots are shown in the logarithmic scale.

## Discussion

Here, we have presented a longitudinal FSI investigation involving six patients with native radio-cephalic AVF.

We found that AVFs that maintained proper patency over time exhibited negligible high-frequency content in the fluid velocity and wall displacement spectrograms throughout the whole investigation period. In contrast, vascular wall vibrations at high frequencies were consistently present in all AVFs that developed complications, whether due to stenosis development or excessive dilatation. Specifically, high-frequency wall vibrations were prominent at the timepoint prior to stenosis or excessive dilatation onset, suggesting a possible relation with adverse vascular remodeling. Among the AVFs with complications, the spectrograms of those that developed stenosis exhibited distinctive features compared to those with excessive venous dilatation. Specifically, patients who developed intimal hyperplasia exhibited two prominent narrow bands (in the 45-65 Hz and 70-100 Hz ranges) in the wall displacement spectrogram before inward remodeling occurred. These bands further increased in frequency and decreased in amplitude after the onset of stenosis, likely due to vessel narrowing and blood flow reduction, respectively. In contrast, patients who experienced excessive dilatation exhibited a single, prominent narrow band at a lower frequency (around 50 Hz) before remodeling. This suggests that different frequency levels may be associated with distinct types of vascular remodeling.

The evolution of vibration amplitudes in AVFs over time and the relation with clinical outcomes also deserves consideration. Patients S1 and S2 exhibited increased vibration amplitudes prior to the formation of stenosis. These amplitudes were damped after vascular remodeling, which can likely be attributed to the laminarization of flow and the reduction in blood flow volume observed following lumen occlusion<sup>35</sup>. However, the amplitudes detected

at 1 year were not completely damped and remained relatively high, suggesting that inward remodeling may have continued over time. Notably, both patients experienced AVF failure a few months after the last follow-up of this investigation, as verified from their medical records. Although we acknowledge that medical images were available only for the intermediate stenosis stage, the persistence of elevated vibration amplitudes may indicate a progressive pathological process. Patient D1 also experienced an attenuation of vibration amplitudes after remodeling, although this occurred following significant dilatation of the JAV. Unlike stenotic AVFs, in this one - in which blood flow remained markedly high - the attenuation of vibrations could be attributed to a substantial decrease in blood velocity, resulting from extreme dilatation. After the current investigation ended, patient D1 underwent transplantation, and the observed attenuation of vibrations suggests that the JAV may not have experienced further dilatation. No complications with the AVF were reported in his clinical records after transplantation. In contrast, patient D2 exhibited increasing AVF vibration amplitudes from maturation to the last follow-up, indicating that dilatation near the JAV curvature may have continued to progress over time. Following the transplant, received a few months after this investigation ended, the AVF experienced further dilatation, as expected, and was eventually closed due to the risk of cardiac overload. Thus, the analysis of AVF vibration amplitude evolution over time suggests that higher vibration amplitudes may indicate future prominent vascular remodeling, while this amplitude is reduced after remodeling occurs.

These observations were supported by statistical analysis. Indeed, we found that AVFs in the 'Adverse Remodeling' group exhibited significantly higher vibration amplitudes and strain before remodeling, compared to those in the 'Patency' group. Significant differences in high-pass strain were observed between the 'Patency' and 'Stenosis' groups, as well as between the 'Patency' and 'Dilatation' groups. Additionally, a significantly higher vibration amplitude

was observed in stenotic patients compared to those with proper patency. However, the difference between ‘Patency’ and ‘Dilatation’ was not statistically significant after Bonferroni correction, suggesting that while increased vibration amplitudes may be linked to excessive dilatation, the relationship appears to be less pronounced compared to that in stenotic AVFs. Thus, the results suggest that specific vibration frequencies and amplitudes are associated with distinct types of vascular remodeling, despite the limited number of patients involved.

The correlation analysis between vibrations and WSS parameters showed that only SPI exhibited a strong and significant association. This finding is plausible, since vascular vibrations are flow-induced, and is consistent with the definition of SPI, which was specifically designed to describe turbulent-like flows and incorporates frequency-based contributions in its formulation <sup>42</sup>. In contrast, the most commonly used TAWSS and OSI showed weaker correlations, indicating limited association with wall vibrations.

The principal limitation of this work is its small sample size, dictated by data acquisition and computational constraints. Although considerable for *in silico* studies, the number of cases remains limited from a clinical perspective, potentially affecting the generalizability of the findings. Moreover, due to patient heterogeneity, we could not assess the impact of comorbidities or baseline vessel sizes on the outcomes. Future studies including larger cohorts would enable more robust statistical analyses and help validate the present preliminary observations.

Moreover, it should be noted that none of the AVFs in this cohort experienced early maturation failure; therefore, no association between vibration patterns and early failure could be established.

Finally, while our simulations reproduced vibration amplitudes consistent with those measured in experimental setups<sup>43,44</sup>, we acknowledge the need for future rigorous validation of the FSI outcomes through in vivo or in vitro studies that replicate patient-specific AVF geometries.

From a mechanobiological perspective, after decades of studies attempting to link WSS on the endothelium to AVF failure<sup>45</sup>, we have demonstrated, for the first time, that flow-induced high-frequency vibrations may play a role in the process of vascular wall remodeling in AVFs. Although most experimental studies have focused on stable or oscillatory flow on endothelial cells<sup>46,47</sup>, our findings align with the little evidence that has been reported in the literature showing that high-frequency mechanical stimuli can influence cellular phenotypes and gene expression in both endothelial and vascular smooth muscle cells, leading to structural and functional changes<sup>32</sup>. These changes include alterations in cytoskeletal organization<sup>48</sup>, disruption of the internal elastic lamina<sup>49-51</sup>, cell proliferation<sup>51-53</sup>, the production of signaling factors, and the activation of pathways related to inflammation, oxidative stress, and vascular dysfunction<sup>54-57</sup>, all of which could have contributed to the adverse vascular remodeling of the AVF we observed in this work. Key effectors and signaling pathways, such as ERK1/2<sup>58</sup>, that lead to intimal thickening and recruitment of inflammatory cells to damaged vessel sites, Syn4, VEGF, KLF2<sup>59</sup>, ICAM-1<sup>49</sup>, and NFATc3<sup>50</sup> have been identified in responding to high-frequency vibrations. Furthermore, high-frequency vibrations have been found to influence muscle atrophy pathways<sup>48</sup>, potentially leading to hypertrophic growth of skeletal muscle which could explain stenosis development occurring in vascular diseases.

The research presented in this work holds significant translational value. Indeed, if the influence of high-frequency mechanical stimuli on AVF failure is confirmed in larger cohorts, this could have significant implications for improving clinical practice and AVF surveillance,

as vibrations may serve as early indicators of complications. Notably, the vibrations detected by FSI simulations in our work, as described here, can easily be felt in the arms of patients with AVF. Some nurses and clinicians currently monitor AVF function based on qualitative assessments of these skin vibrations, the AVF thrill, and by listening to associated sounds with a stethoscope <sup>2</sup>. However, these methods are subjective and rely heavily on the clinician's experience and judgment, underscoring the need for more objective criteria. In this regard, defining specific vibration frequency and amplitude levels through FSI simulations could provide critical insights for clinical practice, identifying thresholds that could serve as biomarkers for different types of vascular remodeling. In the future, if confirmed, the outcomes of this research could pave the way for a rapid, non-invasive, and cost-effective device capable of quantifying vessel vibration amplitudes and related frequencies. Such a device could provide continuous and objective monitoring of AVFs, significantly enhancing surveillance and allowing for the timely identification of patients at risk of developing complications. Moreover, this research could inspire the design of novel devices that would aim to mechanically limit AVF wall vibrations, and promote surgical techniques for creating AVF configurations that minimize the onset of wall vibrations.

This work highlighted the relationship between flow-induced vascular wall vibrations and AVF remodeling and failure. Our preliminary findings revealed that specific vibration frequencies and amplitude levels were associated with distinct types of vascular remodeling, suggesting their potential role in the mechanobiology of vascular cells and as biomarkers for AVF surveillance. Future studies involving larger cohorts will be essential to confirm these findings.

## **Acknowledgments**

The simulations were performed on the Saga cluster, with resources provided by UNINETT Sigma2 – the National Infrastructure for High Performance Computing and Data Storage in Norway, grant number nn9249k. Part of this research was funded by Fondazione Terzi Albini. Luca Soliveri acknowledges a research fellowship received from Fondazione Dompè. The authors would like to thank Dr David Bruneau, Dr Johannes Ring, and Dr. Kei Yamamoto for fruitful discussions.

ACCEPTED

## References

1. Drew DA, Lok CE, Cohen JT, Wagner M, Tangri N, Weiner DE. Vascular Access Choice in Incident Hemodialysis Patients: A Decision Analysis. *JASN*. 2015;26(1):183-191. doi:10.1681/ASN.2013111236
2. Lok CE, Huber TS, Lee T, et al. KDOQI Clinical Practice Guideline for Vascular Access: 2019 Update. *American Journal of Kidney Diseases*. 2020;75(4):S1-S164. doi:10.1053/j.ajkd.2019.12.001
3. Al-Jaishi AA, Oliver MJ, Thomas SM, et al. Patency Rates of the Arteriovenous Fistula for Hemodialysis: A Systematic Review and Meta-analysis. *American Journal of Kidney Diseases*. 2014;63(3):464-478. doi:10.1053/j.ajkd.2013.08.023
4. Caroli A, Manini S, Antiga L, et al. Validation of a patient-specific hemodynamic computational model for surgical planning of vascular access in hemodialysis patients. *Kidney International*. 2013;84(6):1237-1245. doi:10.1038/ki.2013.188
5. Bozzetto M, Poloni S, Caroli A, et al. The use of AVF.SIM system for the surgical planning of arteriovenous fistulae in routine clinical practice. *J Vasc Access*. Published online January 6, 2022:112972982110626. doi:10.1177/11297298211062695
6. Roy-Chaudhury P, Arend L, Zhang J, et al. Neointimal Hyperplasia in Early Arteriovenous Fistula Failure. *American Journal of Kidney Diseases*. 2007;50(5):782-790. doi:10.1053/j.ajkd.2007.07.019
7. Viecelli AK, Mori TA, Roy-Chaudhury P, et al. The pathogenesis of hemodialysis vascular access failure and systemic therapies for its prevention: Optimism unfulfilled. *Semin Dial*. 2018;31(3):244-257. doi:10.1111/sdi.12658
8. Sabiu G, Gallieni M. Pathophysiology of Arteriovenous Fistula Maturation and Nonmaturation. *CJASN*. 2023;18(1):8-10. doi:10.2215/CJN.13101122
9. Sivanesan S. Sites of stenosis in AV fistulae for haemodialysis access. *Nephrology Dialysis Transplantation*. 1999;14(1):118-120. doi:10.1093/ndt/14.1.118
10. Lee T, Roy-Chaudhury P. Advances and new frontiers in the pathophysiology of venous neointimal hyperplasia and dialysis access stenosis. *Adv Chronic Kidney Dis*. 2009;16(5):329-338. doi:10.1053/j.ackd.2009.06.009
11. Roy-Chaudhury P, Sukhatme VP, Cheung AK. Hemodialysis Vascular Access Dysfunction: A Cellular and Molecular Viewpoint. *Journal of the American Society of Nephrology*. 2006;17(4):1112. doi:10.1681/ASN.2005050615
12. Mitra AK, Gangahar DM, Agrawal DK. Cellular, molecular and immunological mechanisms in the pathophysiology of vein graft intimal hyperplasia. *Immunology & Cell Biology*. 2006;84(2):115-124. doi:10.1111/j.1440-1711.2005.01407.x
13. Sequeira A, Tan TW. Complications of a High-flow Access and Its Management. *Seminars in Dialysis*. 2015;28(5):533-543. doi:10.1111/sdi.12366

14. Sigovan M, Rayz V, Gasper W, Alley HF, Owens CD, Saloner D. Vascular Remodeling in Autogenous Arterio-Venous Fistulas by MRI and CFD. *Ann Biomed Eng.* 2013;41(4):657-668. doi:10.1007/s10439-012-0703-4
15. Carroll GT, McGloughlin TM, Burke PE, Egan M, Wallis F, Walsh MT. Wall Shear Stresses Remain Elevated in Mature Arteriovenous Fistulas: A Case Study. *Journal of Biomechanical Engineering.* 2011;133(021003). doi:10.1115/1.4003310
16. Ene-lordache B, Semperboni C, Dubini G, Remuzzi A. Disturbed flow in a patient-specific arteriovenous fistula for hemodialysis: Multidirectional and reciprocating near-wall flow patterns. *Journal of Biomechanics.* 2015;48(10):2195-2200. doi:10.1016/j.jbiomech.2015.04.013
17. Bozzetto M, Ene-lordache B, Remuzzi A. Transitional Flow in the Venous Side of Patient-Specific Arteriovenous Fistulae for Hemodialysis. *Ann Biomed Eng.* 2016;44(8):2388-2401. doi:10.1007/s10439-015-1525-y
18. He Y, Shiu YT, Imrey P, et al. Association of Shear Stress with Subsequent Lumen Remodeling in Hemodialysis Arteriovenous Fistulas. *CJASN.* Published online November 29, 2022:CJN.04630422. doi:10.2215/CJN.04630422
19. Ng O, Thomas S, Gunasekera S, Varcoe R, Barber T. Identifying problematic arteriovenous fistula with CFD-derived resistance: An exploratory study. *Journal of Biomechanics.* 2024;171:112203. doi:10.1016/j.jbiomech.2024.112203
20. Decorato I, Kharboutly Z, Vassallo T, Penrose J, Legallais C, Salsac AV. Numerical simulation of the fluid structure interactions in a compliant patient-specific arteriovenous fistula: FLUID STRUCTURE INTERACTION SIMULATION IN AN ARTERIOVENOUS FISTULA. *Int J Numer Meth Biomed Engng.* 2014;30(2):143-159. doi:10.1002/cnm.2595
21. McGah PM, Leotta DF, Beach KW, Aliseda A. Effects of wall distensibility in hemodynamic simulations of an arteriovenous fistula. *Biomech Model Mechanobiol.* 2014;13(3):679-695. doi:10.1007/s10237-013-0527-7
22. Marcinno' F, Vergara C, Giovannacci L, Quarteroni A, Prouse G. Computational fluid-structure interaction analysis of the end-to-side radio-cephalic arteriovenous fistula. *Computer Methods and Programs in Biomedicine.* Published online April 2024:108146. doi:10.1016/j.cmpb.2024.108146
23. Northrup H, He Y, Berceli S, Cheung AK, Shiu YT. Arteriovenous Fistula Histology, Hemodynamics, and Wall Mechanics: A Case Report of Successful and Failed Access in a Single Patient. *Kidney Medicine.* 2024;6(4):100801. doi:10.1016/j.xkme.2024.100801
24. Jodko D, Barber T. Fluid–structure interaction in a follow-up study of arterio-venous fistula maturation. *Sci Rep.* 2024;14(1):29654. doi:10.1038/s41598-024-80916-y
25. He Y, Wei G, Greene T, et al. Hemodynamics are associated with subsequent lumen remodeling and clinical maturation of hemodialysis arteriovenous fistula. *Sci Rep.* 2025;15(1):6131. doi:10.1038/s41598-025-89896-z
26. Colley E, Carroll J, Anne S, Shannon T, Ramon V, Tracie B. A longitudinal study of the arterio-venous fistula maturation of a single patient over 15 weeks. *Biomech Model Mechanobiol.* 2022;21(4):1217-1232. doi:10.1007/s10237-022-01586-1

27. Bozzetto M, Remuzzi A, Valen-Sendstad K. Flow-induced high frequency vascular wall vibrations in an arteriovenous fistula: a specific stimulus for stenosis development? *Phys Eng Sci Med*. 2024;47(1):187-197. doi:10.1007/s13246-023-01355-z
28. Soliveri L, Bruneau D, Ring J, Bozzetto M, Remuzzi A, Valen-Sendstad K. Toward a physiological model of vascular wall vibrations in the arteriovenous fistula. *Biomech Model Mechanobiol*. 2024;23(5):1741-1755. doi:10.1007/s10237-024-01865-z
29. Soliveri L, Poloni S, Brambilla P, et al. High-Frequency Vessel Wall Vibrations Associate With Stenosis Formation and Arteriovenous Fistula Failure. *Kidney Medicine*. 2025;7(3):100957. doi:10.1016/j.xkme.2024.100957
30. Poloni S, Condemni CG, Peracchi T, Caroli A, Remuzzi A, Bozzetto M. Leveraging Acoustic Analysis to Detect Arteriovenous Fistula Complications. *Kidney360*. Published online February 25, 2025:10.34067/KID.0000000840. doi:10.34067/KID.0000000840
31. Poloni S, Soliveri L, Caroli A, Remuzzi A, Bozzetto M. The Potential of Sound Analysis to Reveal Hemodynamic Conditions of Arteriovenous Fistulae for Hemodialysis. *Ann Biomed Eng*. 2025;53(1):230-240. doi:10.1007/s10439-024-03638-2
32. Carrara E, Soliveri L, Poloni S, Bozzetto M, Campiglio CE. Effects of high-frequency mechanical stimuli on flow related vascular cell biology. *Int J Artif Organs*. Published online August 21, 2024:03913988241268105. doi:10.1177/03913988241268105
33. Bozzetto M, Brambilla P, Rota S, et al. Toward longitudinal studies of hemodynamically induced vessel wall remodeling. *Int J Artif Organs*. 2018;41(11):714-722. doi:10.1177/0391398818784207
34. Bozzetto M, Soliveri L, Poloni S, et al. Arteriovenous fistula creation with VasQ™ device: A feasibility study to reveal hemodynamic implications. *J Vasc Access*. Published online April 22, 2022:112972982210871. doi:10.1177/11297298221087160
35. Soliveri L, Bozzetto M, Brambilla P, Caroli A, Remuzzi A. Hemodynamics in AVF over time: A protective role of vascular remodeling toward flow stabilization. *Int J Artif Organs*. 2023;46(10-11):547-554. doi:10.1177/03913988231191960
36. Bergersen A, Slyngstad A, Gjertsen S, Souche A, Valen-Sendstad K. turtleFSI: A Robust and Monolithic FEniCS-based Fluid-Structure Interaction Solver. *JOSS*. 2020;5(50):2089. doi:10.21105/joss.02089
37. Khan MO, Valen-Sendstad K, Steinman DA. Narrowing the Expertise Gap for Predicting Intracranial Aneurysm Hemodynamics: Impact of Solver Numerics versus Mesh and Time-Step Resolution. *American Journal of Neuroradiology*. 2015;36(7):1310-1316. doi:10.3174/ajnr.A4263
38. Remuzzi A, Bozzetto M. Biological and Physical Factors Involved in the Maturation of Arteriovenous Fistula for Hemodialysis. *Cardiovasc Eng Tech*. 2017;8(3):273-279. doi:10.1007/s13239-017-0323-0
39. Moireau P, Xiao N, Astorino M, et al. External tissue support and fluid–structure simulation in blood flows. *Biomech Model Mechanobiol*. 2012;11(1-2):1-18. doi:10.1007/s10237-011-0289-z

40. Natarajan T, MacDonald DE, Najafi M, Khan MO, Steinman DA. On the spectrographic representation of cardiovascular flow instabilities. *Journal of Biomechanics*. 2020;110:109977. doi:10.1016/j.jbiomech.2020.109977
41. Bruneau DA, Steinman DA, Valen-Sendstad K. Understanding intracranial aneurysm sounds via high-fidelity fluid-structure-interaction modelling. *Commun Med*. 2023;3(1):163. doi:10.1038/s43856-023-00396-5
42. Khan MO, Chnafa C, Gallo D, et al. On the quantification and visualization of transient periodic instabilities in pulsatile flows. *Journal of Biomechanics*. 2017;52:179-182. doi:10.1016/j.jbiomech.2016.12.037
43. Foreman JEK, Hutchison KJ. Arterial Wall Vibration Distal to Stenoses in Isolated Arteries of Dog and Man. *Circulation Research*. 1970;26(5):583-590. doi:10.1161/01.RES.26.5.583
44. Fillinger MF, Reinitz ER, Schwartz RA, et al. Graft geometry and venous intimal-medial hyperplasia in arteriovenous loop grafts. 1990;11(4).
45. Colley E, Simmons A, Varcoe R, Thomas S, Barber T. Arteriovenous fistula maturation and the influence of fluid dynamics. *Proc Inst Mech Eng H*. 2020;234(11):1197-1208. doi:10.1177/0954411920926077
46. Brahmabhatt A, Remuzzi A, Franzoni M, Misra S. The molecular mechanisms of hemodialysis vascular access failure. *Kidney International*. 2016;89(2):303-316. doi:10.1016/j.kint.2015.12.019
47. Franzoni M, Cattaneo I, Longaretti L, Figliuzzi M, Ene-Iordache B, Remuzzi A. Endothelial cell activation by hemodynamic shear stress derived from arteriovenous fistula for hemodialysis access. *American Journal of Physiology-Heart and Circulatory Physiology*. 2016;310(1):H49-H59. doi:10.1152/ajpheart.00098.2015
48. Ceccarelli G, Benedetti L, Galli D, et al. Low-amplitude high frequency vibration down-regulates myostatin and atrogin-1 expression, two components of the atrophy pathway in muscle cells. *J Tissue Eng Regen Med*. 2014;8(5):396-406. doi:10.1002/term.1533
49. Krajnak K, Miller GR, Waugh S. Contact area affects frequency-dependent responses to vibration in the peripheral vascular and sensorineural systems. *J Toxicol Environ Health A*. 2018;81(1-3):6-19. doi:10.1080/15287394.2017.1401022
50. Curry BD, Bain JLW, Yan JG, et al. Vibration injury damages arterial endothelial cells. *Muscle & Nerve*. 2002;25(4):527-534. doi:10.1002/mus.10058
51. Inaba R, Furuno T, Okada A. Effects of low- and high-frequency local vibration on the occurrence of intimal thickening of the peripheral arteries of rats. *Scand J Work Environ Health*. 1988;14(5):312-316. doi:10.5271/sjweh.1914
52. Okada A, Inaba R, Furuno T, Nohara S, Ariizumi M. Usefulness of blood parameters, especially viscosity, for the diagnosis and elucidation of pathogenic mechanisms of the hand-arm vibration syndrome. *Scandinavian Journal of Work, Environment & Health*. 1987;13(4):358-362. doi:10.5271/sjweh.2027
53. Bittle BB. *An Investigation into the Role of Arterial Wall Vibration in the Pathogenesis of Atherosclerosis*. Doctor of Philosophy. Iowa State University, Digital Repository; 1994. doi:10.31274/rtd-180813-12262

54. Cao W, Zhang D, Li Q, et al. Biomechanical Stretch Induces Inflammation, Proliferation, and Migration by Activating NFAT5 in Arterial Smooth Muscle Cells. *Inflammation*. 2017;40(6):2129-2136. doi:10.1007/s10753-017-0653-y
55. Wang Y, Cao W, Cui J, et al. Arterial Wall Stress Induces Phenotypic Switching of Arterial Smooth Muscle Cells in Vascular Remodeling by Activating the YAP/TAZ Signaling Pathway. *Cell Physiol Biochem*. 2018;51(2):842-853. doi:10.1159/000495376
56. Krajnak K, Miller GR, Waugh S, Johnson C, Li S, Kashon ML. Characterization of frequency-dependent responses of the vascular system to repetitive vibration. *J Occup Environ Med*. 2010;52(6):584-594. doi:10.1097/JOM.0b013e3181e12b1f
57. Mu L, Sun A, Chen Y, et al. Vascular response to the microcirculation in the fingertip by local vibration with varied amplitude. *Front Bioeng Biotechnol*. 2023;11. doi:10.3389/fbioe.2023.1197772
58. Loth F, Fischer PF, Arslan N, et al. Transitional Flow at the Venous Anastomosis of an Arteriovenous Graft: Potential Activation of the ERK1/2 Mechanotransduction Pathway. *Journal of Biomechanical Engineering*. 2003;125(1):49-61. doi:10.1115/1.1537737
59. Uryash A, Adams JA. Abstract 18011: Vibroacoustic Noninvasive Stimulation (VATS) of Human Coronary Endothelial Cells Induced Syndecan-4, VEGF and KLF2 Mechanosensor Control of eNOS. *Circulation*. 2017;136(suppl\_1):A18011-A18011. doi:10.1161/circ.136.suppl\_1.18011

**Table 1.** Clinical data for the six patients involved.

	<b>P1</b>	<b>P2</b>	<b>S1</b>	<b>S2</b>	<b>D1</b>	<b>D2</b>
<b>Weight (kg)</b>	78	67	68	93	77	66
<b>Height (cm)</b>	170	162	170	163	180	173
<b>Native kidney disease</b>	Unknown	ANCA vasculitis	ADPKD	Hypertensive nephropathy	Unknown	IgA nephropathy
<b>Office blood pressure (mmHg)</b>	150/70	160/90	140/85	125/68	130/85	120/77
<b>Hypertension</b>	Yes	Yes	Yes	Yes	Yes	No
<b>Diabetes</b>	Yes	No	No	No	No	No
<b>Cardiovascular disease</b>	No	No	No	No	No	No
<b>Dialysis modalities at AVF surgery</b>	None	Hemodialysis with CVC	None	None	None	Peritoneal dialysis
<b>AVF access</b>	Left distal radio-cephalic	Left distal radio-cephalic	Left distal radio-cephalic	Left distal radio-cephalic	Right distal radio-cephalic	Left distal radio-cephalic
<b>AVF anastomosis</b>	L-T	L-T	L-T	L-T	L-T	L-T
<b>Time to successful dialysis initiation (days)</b>	33	50	130	43	50	48
<b>BA diameter pre-op (mm)</b>	5.2	4.3	4.7	5.3	4.8	4.6
<b>RA diameter pre-op (mm)</b>	3.3	2.4	3.0	2.6	2.4	2.2
<b>CV diameter pre-op (mm)</b>	3.9	2.8	2.3	2.7	3.0	2.5
<b>BA blood flow pre-op (mL/min)</b>	60	49	20	103	42	32
<b>RA blood flow pre-op (mL/min)</b>	37	23	9	55	22	24
<b>BA diameter 1 year (mm)</b>	5.9	6.6	7.1	6.5	7.1	6.8
<b>RA<sub>prox</sub> diameter 1 year (mm)</b>	4.4	6.0	7.0	5.2	5.5	5.4

<b>RA<sub>dist</sub> diameter 1 year (mm)</b>	3.2	4.8	2.5	3.6	4.2	4.2
<b>CV diameter 1 year (mm)</b>	7.2	8.4	2.0	3.5	14.8	13.1
<b>BA blood flow 1 year (mL/min)</b>	527	840	860	777	1545	801
<b>RA<sub>prox</sub> blood flow 1 year (mL/min)</b>	316	568	520	560	916	582
<b>RA<sub>dist</sub> blood flow 1 year (mL/min)</b>	27	217	4	91	250	112
<b>AVF outcome</b>	Patent	Patent	Stenosis	Stenosis	Excessive dilatation	Excessive dilatation

Abbreviations: ADPKD = autosomal dominant polycystic kidney disease, ANCA = anti-neutrophil cytoplasmic antibody, AVF = arteriovenous fistula, BA = brachial artery, CV = cephalic vein, CVC = central venous catheter, IgA = immunoglobulin A, L-T= latero-terminal, RA = radial artery.

## Figure legends

**Figure 1. a)** Investigation timeline showing the time points at which clinical data acquisition and computational analysis were performed. **b)** Fluid-structure interaction pipeline used to characterize AVF hemodynamics and high-frequency vascular vibrations. Abbreviations: AVF = arteriovenous fistula, DA = distal artery, DUS = Doppler ultrasound, FSI = fluid-structure interaction, MRI = magnetic resonance imaging, PA = proximal artery, V = vein.

ACCEPTED

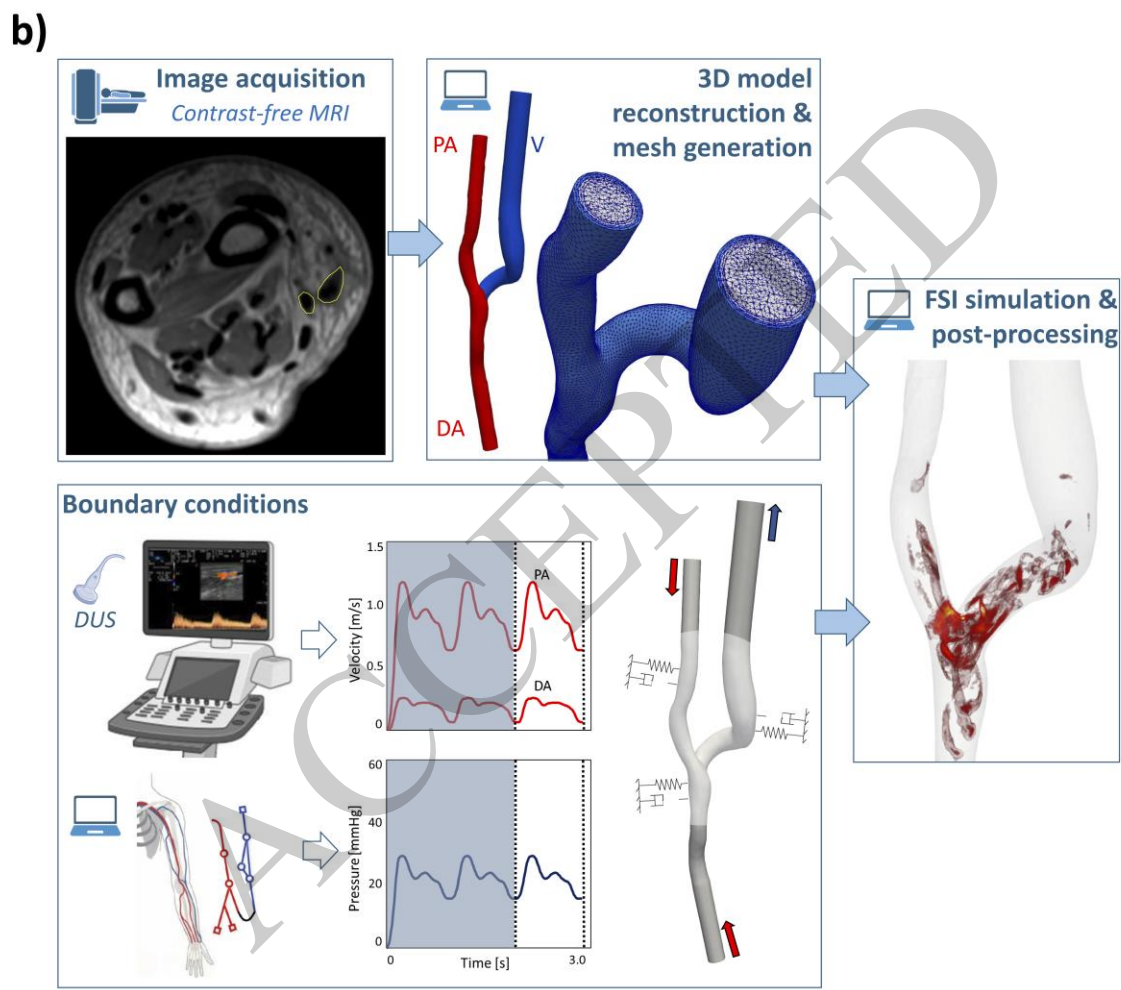
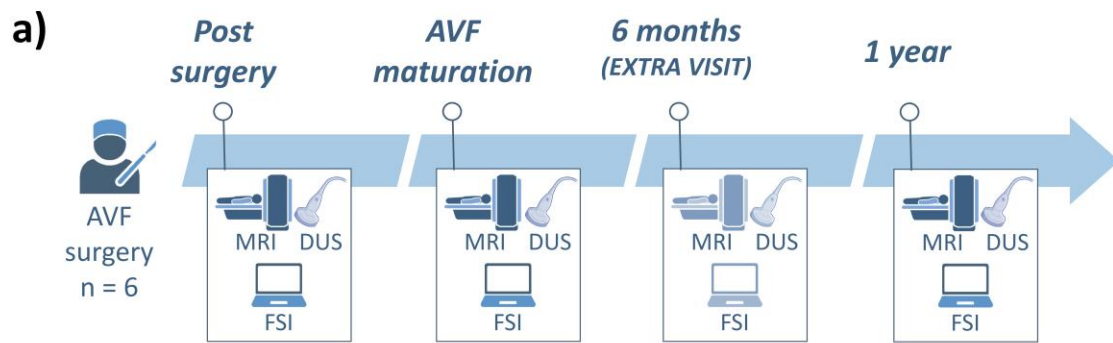


**Figure 2.** Three-dimensional AVF models generated from medical imaging data, with average inlet blood flow rates measured during Doppler ultrasound examinations, for the six AVFs under study, at various time points. Black arrows indicate the direction of blood flow entering the proximal and distal arteries, while red and orange arrows denote locations of stenosis and excessive dilatation, respectively. Abbreviations: D = excessive dilatation, P = patency, S = stenosis.

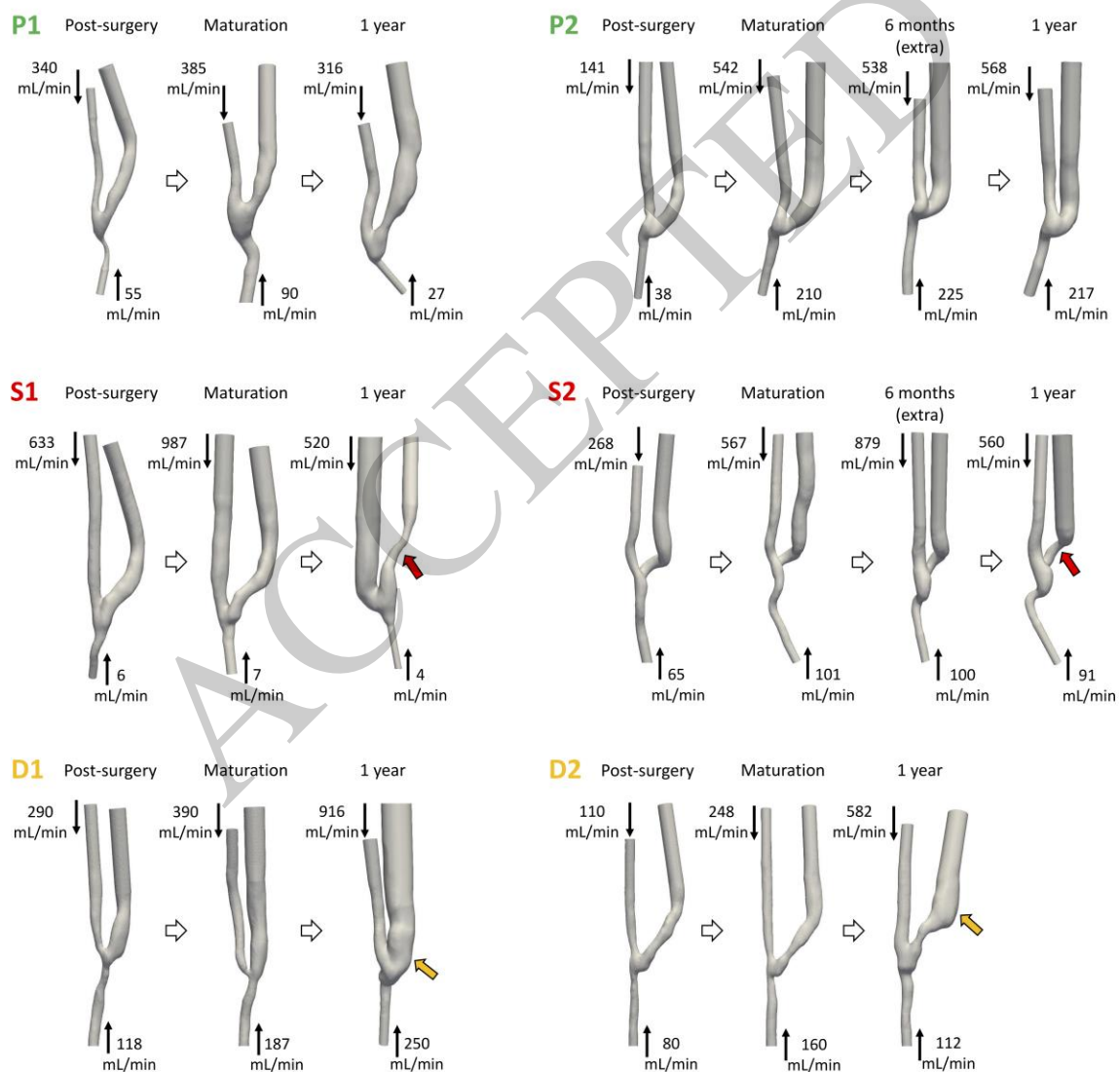


**Figure 3.** Evolution over time of brachial artery, radial artery (proximal and distal), and cephalic vein diameters in the six AVFs under study. The diameters of the radial artery and cephalic vein were measured approximately 2 cm from the anastomosis. The figure also illustrates blood flow volumes entering the vascular access via the brachial artery, as well as through the proximal and distal radial arteries. Abbreviations: D = excessive dilatation, P = patency, S = stenosis.

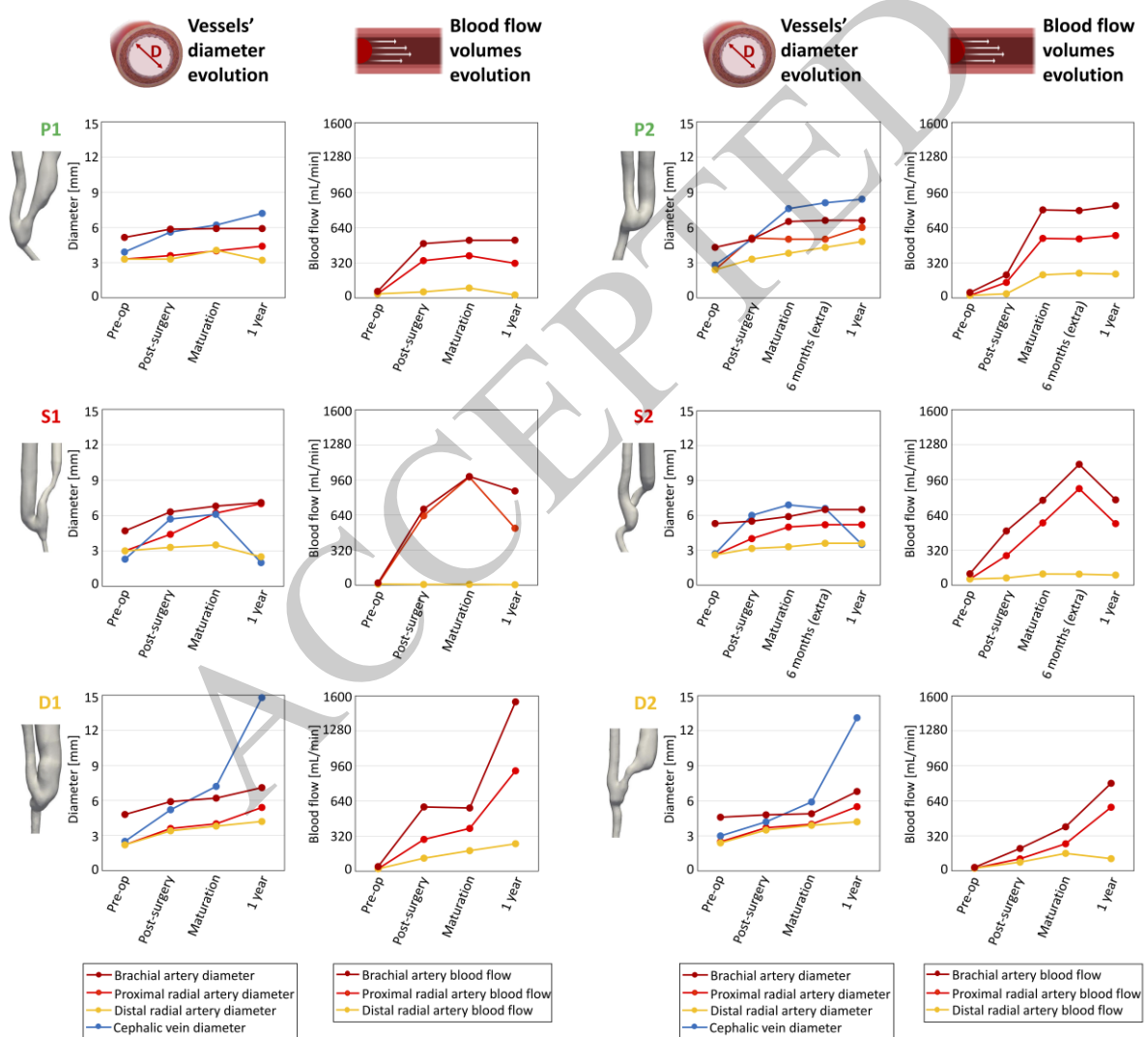


**Figure 4.** Effect of transitional flow on high-frequency velocity fluctuations and vascular wall vibrations in the six AVFs under study, at different time points. For each patient, the first row displays vortex visualization at peak systole using the Q-criterion, the second row shows the fluid velocity spectrograms, and the third row presents the wall displacement spectrograms. Spectrograms were extracted in the juxta-anastomotic vein region. In the spectrograms, dark blue represents low spectral power, while yellow indicates high spectral power. Abbreviations: D = excessive dilatation, P = patency, S = stenosis.

ACCEPTED

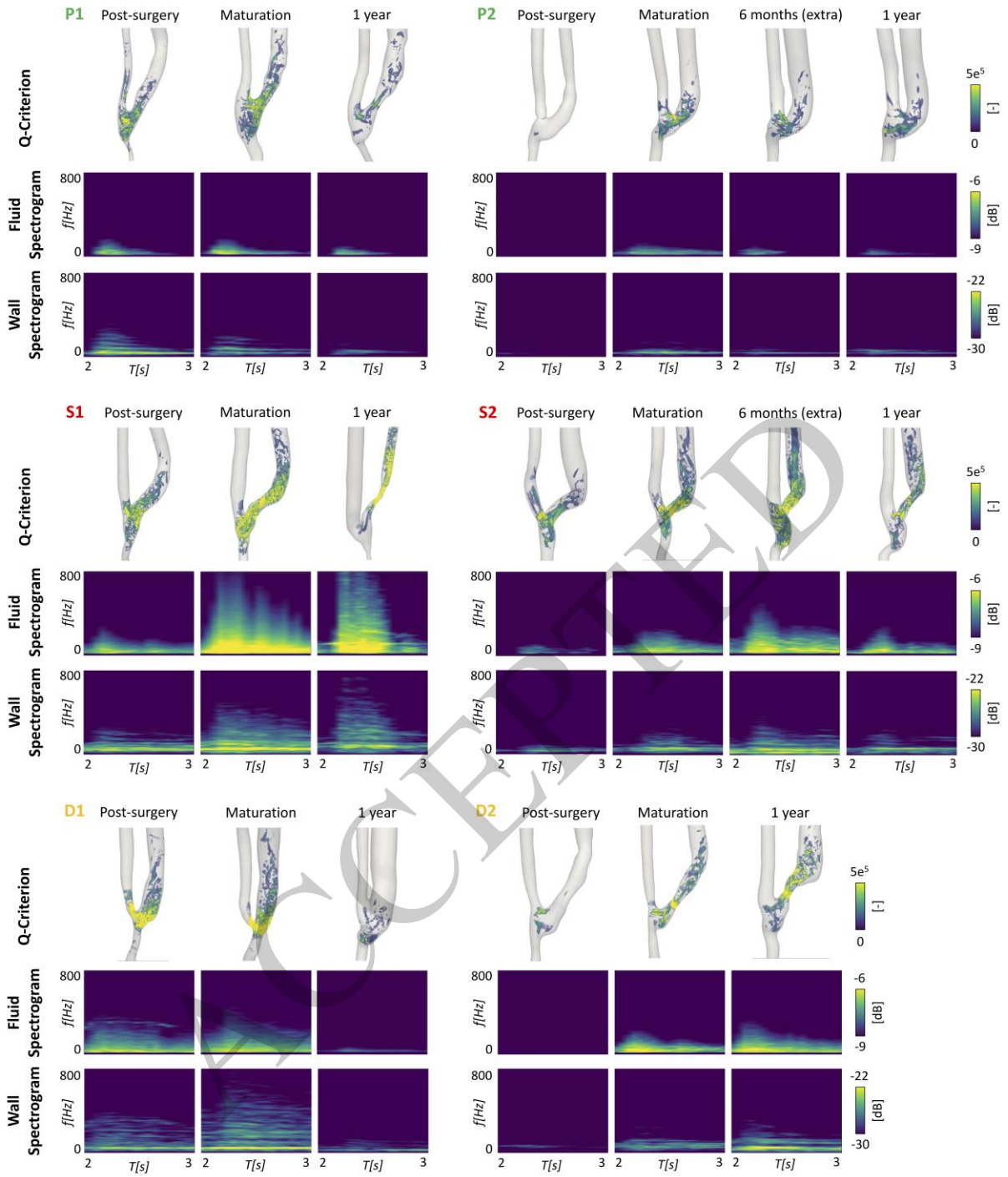


**Figure 5.** Temporal evolution of wall vibration amplitudes throughout a cardiac cycle for the six AVFs under study. The 99<sup>th</sup> spatial percentile of vibration amplitude is used as the representative measure for vibrations. The 3D models in the figure are representative of AVF clinical outcome of the AVF. Abbreviations: D = excessive dilatation, P = patency, S = stenosis.

ACCEPTED

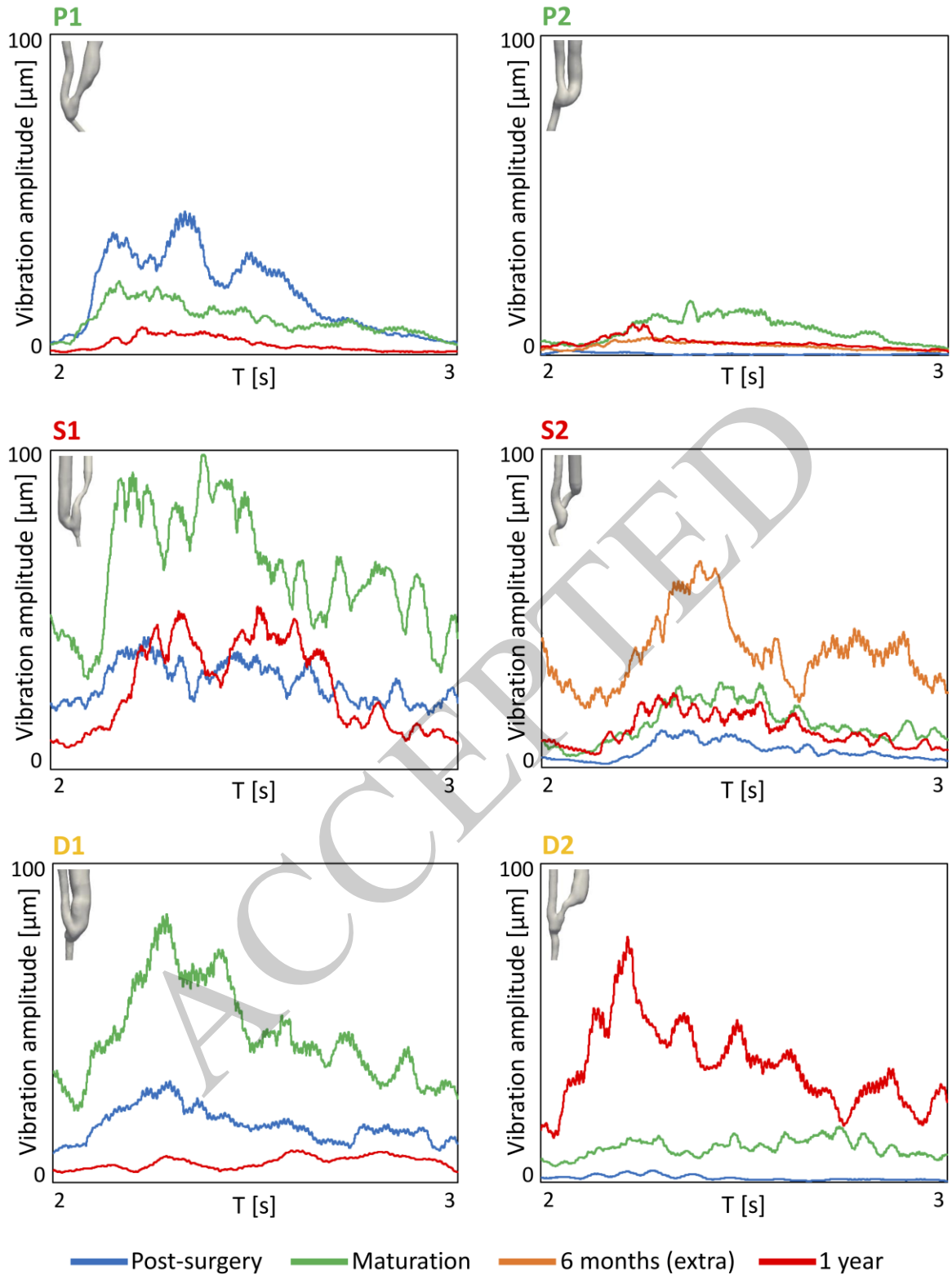


**Figure 6.** Boxplots illustrate differences in the distributions of time-averaged vibration amplitude and high-pass strain across groups. Cross-sectional slices from simulation results, extracted within the first 2.5 cm of the vein with 1 mm slice spacing, were used for statistical analysis. A generalized linear mixed-effects model was fitted, with Vibration amplitude and Strain as the response variables, Group ('Patency', 'Stenosis', and 'Dilatation') as a fixed effect, and Patient as a random effect to account for repeated measures within individual patients. The analysis first combined all patients with adverse remodeling, then distinguished between the 'Stenosis' and excessive 'Dilatation' groups. For comparisons between the three groups, p-values were adjusted using Bonferroni correction. The number of '\*' symbols indicates the difference in levels of significance between groups.

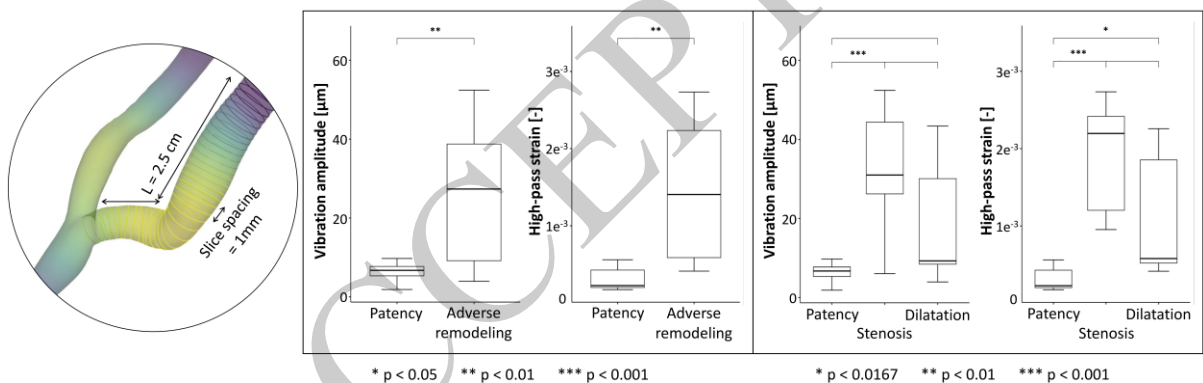
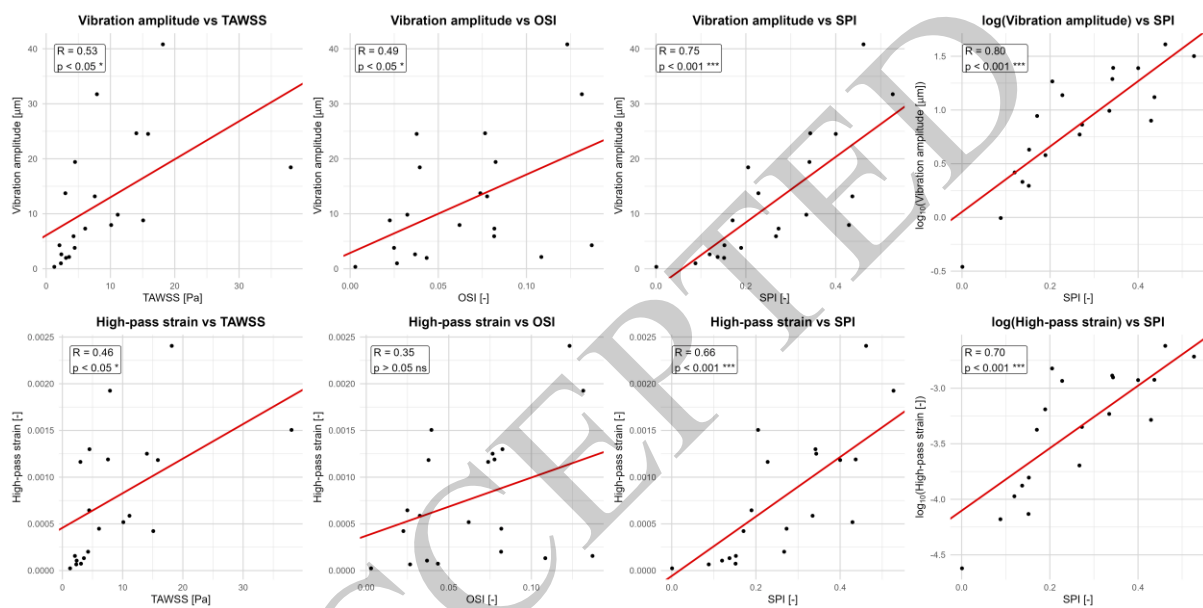


**Figure 7.** Correlations between hemodynamic parameters (TAWSS, OSI, SPI) and vibrations (vibration amplitude and high-pass strain). Each panel shows the linear relationship estimated using mixed-effects models (red line) with patient as a random factor. R values represent conditional correlation coefficients, and p values indicate statistical significance levels ( $p < 0.05$  \*,  $p < 0.01$  \*\*,  $p < 0.001$  \*\*\*). Additional panels display SPI correlations with log-transformed variables, showing slightly improved fits.



## **Supplemental Table of Contents**

Supplemental Methods. Fluid-structure interaction pipeline.


ACCEPTED

# High Frequency Wall Vibrations in Vascular Remodeling of Arteriovenous Fistulas (AVFs)


KIDNEY360<sup>®</sup>

Accessing Our World From Every Angle


Clinical Research



End-stage Kidney Disease Patients  
N = 6




Native distal radio-cephalic AVF




Patients followed up for one year with MRI and DUS

MRI: Magnetic resonance imaging  
DUS: Doppler ultrasound


### AVF Outcomes




2 patients maintained proper AVF patency




4 patients developed complications




Fluid-structure interaction simulations revealed distinct vibration frequency patterns that preceded vascular remodeling with stenotic AVFs showing two dominant bands (45–100 Hz) and excessively dilated AVFs showing a single dominant band around 50 Hz



Before remodeling, patients who later developed complications had significantly higher vibration amplitude compared with those with preserved patency ( $22.5 \pm 5.8 \mu\text{m}$  vs.  $6.6 \pm 2.0 \mu\text{m}$ ,  $p < 0.01$ )



High-pass strain was also significantly elevated prior to remodeling in patients with complications compared with those with proper patency ( $(1.30 \pm 0.35) \times 10^{-3}$  vs.  $(0.30 \pm 0.10) \times 10^{-3}$ ,  $p < 0.01$ ).



Vibration amplitude and high-pass strain effectively discriminated AVF outcomes, distinguishing preserved patency from stenosis and excessive dilatation with strong statistical significance

Conclusions: Distinct vibration frequencies and amplitude levels appear to correlate with specific types of vascular remodeling, indicating their potential utility as biomarkers for AVF surveillance

Luca Soliveri, et al. *The Role of High-Frequency Wall Vibrations in Adverse Vascular Remodeling of Arteriovenous Fistula for Hemodialysis.* *Kidney360.* DOI: 10.34067/KID.0000001112  
Visual Abstract by Hector M Madariaga, MD FASN

ACCEPTED

## ASN Journal Disclosure Form

As per ASN journal policy, I have disclosed any financial relationships or commitments I have held in the past 36 months as included below. I have listed my Current Employer below to indicate there is a relationship requiring disclosure. If no relationship exists, my Current Employer is not listed.

M. Bozzetto has nothing to disclose.

I understand that the information above will be published within the journal article, if accepted, and that failure to comply and/or to accurately and completely report the potential financial conflicts of interest could lead to the following: 1) Prior to publication, article rejection, or 2) Post-publication, sanctions ranging from, but not limited to, issuing a correction, reporting the inaccurate information to the authors' institution, banning authors from submitting work to ASN journals for varying lengths of time, and/or retraction of the published work.

Name: Michela Bozzetto

Manuscript ID: K360-2025-001100

Manuscript Title: The role of high-frequency wall vibrations in adverse vascular remodeling of arteriovenous fistula for hemodialysis

Date of Completion: November 18, 2025

Disclosure Updated Date: February 19, 2025

## ASN Journal Disclosure Form

As per ASN journal policy, I have disclosed any financial relationships or commitments I have held in the past 36 months as included below. I have listed my Current Employer below to indicate there is a relationship requiring disclosure. If no relationship exists, my Current Employer is not listed.

P. Brambilla has nothing to disclose.

I understand that the information above will be published within the journal article, if accepted, and that failure to comply and/or to accurately and completely report the potential financial conflicts of interest could lead to the following: 1) Prior to publication, article rejection, or 2) Post-publication, sanctions ranging from, but not limited to, issuing a correction, reporting the inaccurate information to the authors' institution, banning authors from submitting work to ASN journals for varying lengths of time, and/or retraction of the published work.

Name: Paolo Brambilla

Manuscript ID: K360-2025-001100R1

Manuscript Title: The role of high-frequency wall vibrations in adverse vascular remodeling of arteriovenous fistula for hemodialysis

Date of Completion: November 28, 2025

Disclosure Updated Date: November 28, 2025

## ASN Journal Disclosure Form

As per ASN journal policy, I have disclosed any financial relationships or commitments I have held in the past 36 months as included below. I have listed my Current Employer below to indicate there is a relationship requiring disclosure. If no relationship exists, my Current Employer is not listed.

G. Cabrini reports the following:

Employer: Università degli studi di Bergamo

I understand that the information above will be published within the journal article, if accepted, and that failure to comply and/or to accurately and completely report the potential financial conflicts of interest could lead to the following: 1) Prior to publication, article rejection, or 2) Post-publication, sanctions ranging from, but not limited to, issuing a correction, reporting the inaccurate information to the authors' institution, banning authors from submitting work to ASN journals for varying lengths of time, and/or retraction of the published work.

Name: Giulia Cabrini

Manuscript ID: K360-2025-001100R1

Manuscript Title: The role of high-frequency wall vibrations in adverse vascular remodeling of arteriovenous fistula for hemodialysis

Date of Completion: November 26, 2025

Disclosure Updated Date: November 20, 2025

## ASN Journal Disclosure Form

As per ASN journal policy, I have disclosed any financial relationships or commitments I have held in the past 36 months as included below. I have listed my Current Employer below to indicate there is a relationship requiring disclosure. If no relationship exists, my Current Employer is not listed.

A. Caroli has nothing to disclose.

I understand that the information above will be published within the journal article, if accepted, and that failure to comply and/or to accurately and completely report the potential financial conflicts of interest could lead to the following: 1) Prior to publication, article rejection, or 2) Post-publication, sanctions ranging from, but not limited to, issuing a correction, reporting the inaccurate information to the authors' institution, banning authors from submitting work to ASN journals for varying lengths of time, and/or retraction of the published work.

Name: Anna Caroli

Manuscript ID: K360-2025-001100R1

Manuscript Title: The role of high-frequency wall vibrations in adverse vascular remodeling of arteriovenous fistula for hemodialysis

Date of Completion: November 10, 2025

Disclosure Updated Date: February 19, 2025

## ASN Journal Disclosure Form

As per ASN journal policy, I have disclosed any financial relationships or commitments I have held in the past 36 months as included below. I have listed my Current Employer below to indicate there is a relationship requiring disclosure. If no relationship exists, my Current Employer is not listed.

S. Poloni reports the following:

Employer: University of Bergamo

I understand that the information above will be published within the journal article, if accepted, and that failure to comply and/or to accurately and completely report the potential financial conflicts of interest could lead to the following: 1) Prior to publication, article rejection, or 2) Post-publication, sanctions ranging from, but not limited to, issuing a correction, reporting the inaccurate information to the authors' institution, banning authors from submitting work to ASN journals for varying lengths of time, and/or retraction of the published work.

Name: Sofia Poloni

Manuscript ID: K360-2025-001100R1

Manuscript Title: The role of high-frequency wall vibrations in adverse vascular remodeling of arteriovenous fistula for hemodialysis

Date of Completion: November 11, 2025

Disclosure Updated Date: November 11, 2025

## ASN Journal Disclosure Form

As per ASN journal policy, I have disclosed any financial relationships or commitments I have held in the past 36 months as included below. I have listed my Current Employer below to indicate there is a relationship requiring disclosure. If no relationship exists, my Current Employer is not listed.

A. Remuzzi reports the following:

Employer: University of Bergamo - Italy; Consultancy: Mario Negri Institute, Bergamo - Italy; and Advisory or Leadership Role: The International Journal of Artificial Organs.

I understand that the information above will be published within the journal article, if accepted, and that failure to comply and/or to accurately and completely report the potential financial conflicts of interest could lead to the following: 1) Prior to publication, article rejection, or 2) Post-publication, sanctions ranging from, but not limited to, issuing a correction, reporting the inaccurate information to the authors' institution, banning authors from submitting work to ASN journals for varying lengths of time, and/or retraction of the published work.

Name: Andrea Remuzzi

Manuscript ID: K360-2025-001100R1

Manuscript Title: The role of high-frequency wall vibrations in adverse vascular remodeling of arteriovenous fistula for hemodialysis

Date of Completion: November 18, 2025

Disclosure Updated Date: February 19, 2025

## ASN Journal Disclosure Form

As per ASN journal policy, I have disclosed any financial relationships or commitments I have held in the past 36 months as included below. I have listed my Current Employer below to indicate there is a relationship requiring disclosure. If no relationship exists, my Current Employer is not listed.

L. Soliveri has nothing to disclose.

I understand that the information above will be published within the journal article, if accepted, and that failure to comply and/or to accurately and completely report the potential financial conflicts of interest could lead to the following: 1) Prior to publication, article rejection, or 2) Post-publication, sanctions ranging from, but not limited to, issuing a correction, reporting the inaccurate information to the authors' institution, banning authors from submitting work to ASN journals for varying lengths of time, and/or retraction of the published work.

Name: Luca Soliveri

Manuscript ID: K360-2025-001100R1

Manuscript Title: The role of high-frequency wall vibrations in adverse vascular remodeling of arteriovenous fistula for hemodialysis

Date of Completion: November 10, 2025

Disclosure Updated Date: November 10, 2025

## ASN Journal Disclosure Form

As per ASN journal policy, I have disclosed any financial relationships or commitments I have held in the past 36 months as included below. I have listed my Current Employer below to indicate there is a relationship requiring disclosure. If no relationship exists, my Current Employer is not listed.

K. Valen-Sendstad has nothing to disclose.

I understand that the information above will be published within the journal article, if accepted, and that failure to comply and/or to accurately and completely report the potential financial conflicts of interest could lead to the following: 1) Prior to publication, article rejection, or 2) Post-publication, sanctions ranging from, but not limited to, issuing a correction, reporting the inaccurate information to the authors' institution, banning authors from submitting work to ASN journals for varying lengths of time, and/or retraction of the published work.

Name: Kristian Valen-Sendstad

Manuscript ID: K360-2025-001100R1

Manuscript Title: The role of high-frequency wall vibrations in adverse vascular remodeling of arteriovenous fistula for hemodialysis

Date of Completion: December 11, 2025

Disclosure Updated Date: December 11, 2025

## ASN Journal Disclosure Form

As per ASN journal policy, I have disclosed any financial relationships or commitments I have held in the past 36 months as included below. I have listed my Current Employer below to indicate there is a relationship requiring disclosure. If no relationship exists, my Current Employer is not listed.

S. Zerbi has nothing to disclose.

I understand that the information above will be published within the journal article, if accepted, and that failure to comply and/or to accurately and completely report the potential financial conflicts of interest could lead to the following: 1) Prior to publication, article rejection, or 2) Post-publication, sanctions ranging from, but not limited to, issuing a correction, reporting the inaccurate information to the authors' institution, banning authors from submitting work to ASN journals for varying lengths of time, and/or retraction of the published work.

Name: Simona Zerbi

Manuscript ID: K360-2025-001100R1

Manuscript Title: The role of high-frequency wall vibrations in adverse vascular remodeling of arteriovenous fistula for hemodialysis

Date of Completion: November 18, 2025

Disclosure Updated Date: November 18, 2025